Journal of the American College of Cardiology
© 2007 by the American College of Cardiology Foundation
Published by Elsevier Inc.

Vol. 49, No. 25, 2007
ISSN 0735-1097/07/$32.00
doi:10.1016/j.jacc.2007.02.060

PRECLINICAL STUDY

Potentiation of Doxorubicin Cardiotoxicity by Iron Loading in a Rodent Model

Gurusher S. Panjrath, MD,* Virender Patel, MD,* Carolina I. Valdiviezo, MD,‡ Navneet Narula, MD,† Jagat Narula, MD, PhD, FACC,* Diwakar Jain, MD, FACC*

Philadelphia, Pennsylvania; and New York, New York

Objectives The role of iron toward doxorubicin (DOX) cardiotoxicity was studied using a rodent model of dietary carbonyl iron loading.

Background Doxorubicin, a commonly used anticancer drug, is known to cause serious and potentially life-threatening cardiotoxicity. Doxorubicin cardiotoxicity is thought to be mediated through free-radical injury.

Methods Male Sprague Dawley rats fed iron-rich chow (n = 8) and regular chow (n = 8) were treated with DOX or saline (4 animals in each arm). Cardiotoxicity was assessed using mortality, weight changes, Tc-99m annexin-V imaging, histopathology, and immunohistochemistry.

Results Animals fed iron-rich chow showed significantly higher DOX cardiotoxicity as evidenced by greater weight loss (107 ± 14 g vs. 55 ± 10 g weight loss, $p < 0.05$), higher annexin uptake (0.14 ± 0.01% vs. 0.08 ± 0.01% injected dose/g of myocardium, $p < 0.05$), more severe myocyte injury on electron microscopy, and significantly higher cleaved caspase-3 staining compared with regular chow fed rats given DOX. Feeding iron-rich chow alone did not result in any cardiotoxicity.

Conclusions Dietary iron loading resulted in a substantially increased DOX cardiotoxicity in rats. Body iron stores as well as its bioavailability in tissue may be important independent predictors of susceptibility to DOX cardiotoxicity in man. Further clinical studies are warranted. (J Am Coll Cardiol 2007;49:2457–64) © 2007 by the American College of Cardiology Foundation

Doxorubicin (DOX), a potent anthracycline antineoplastic agent, is used widely in a variety of malignancies and tumors (1–3). Despite being one of the most effective anticancer agents, its use is limited by serious and sometimes life-threatening cardiotoxicity (4,5). Despite extensive studies in animals and cell culture models, the exact cellular, biochemical, molecular, and genetic mechanism of DOX cardiotoxicity is not fully known. Advanced age, concomitant treatment with radiation therapy, or high-dose cyclophosphamide and pre-existing heart disease have been identified as predisposing factors for DOX cardiotoxicity (4,6). However, these factors alone cannot explain the wide variation in individual susceptibility to DOX cardiotoxicity.

Redox injury and interference with protein synthesis are considered to play a significant role in DOX cardiotoxicity (7–9). Conditions that exacerbate free-radical formation may enhance DOX cardiotoxicity. Various studies have proposed a role of metallic ions in DOX-mediated damage (10–12). Doxorubicin interacts with metallic ions, especially iron, which results in the formation of DOX-iron (III) complex (13–15). Iron independently plays an important role in generation of harmful free radicals with potential deleterious effects on the myocardium. Iron chelator dexrazoxane is recommended for use in patients receiving higher doses of DOX to prevent heart failure (16,17). Despite these measures, cardiotoxicity continues to be an important limiting factor for DOX therapy.

We have aimed to elucidate the role of iron in potentiation of DOX-induced cardiotoxicity. We hypothesize that elevated body iron content enhances the cardiotoxic effects of DOX. We used an in-vivo rodent model of nutritional iron loading, which may simulate patterns of higher body iron stores observed in patients undergoing cancer chemotherapy.

Methods

Animals. Male Sprague Dawley rats (Charles River Laboratories, Wilmington, Massachusetts) were used in accordance with guidelines on animal care. The study was

From the *Division of Cardiology, Drexel University College of Medicine, Philadelphia, Pennsylvania; †Pathology Department, University of Pennsylvania, Philadelphia, Pennsylvania; and the ‡Cardiovascular Biology Research Laboratory, Mount Sinai School of Medicine, New York, New York. Supported by the American Society of Nuclear Cardiology/Fujisawa Healthcare Award, Bethesda, Maryland.

Manuscript received December 4, 2006; revised manuscript received January 24, 2007, accepted February 6, 2007.

Abbreviations and Acronyms

DOX = doxorubicin

HFE = iron regulatory gene

approved by the institutional animal care committee. The animals received a single intravenous dose of DOX. Further division was based on those fed regular rat chow or those fed iron-rich chow. Each group had a corresponding saline-treated control. Figure 1 demonstrates the various study groups. There were 4 animals in each of the 4 study groups. A pilot group of 5 animals was initially tested for dosage and was not included for hypothesis testing.

Dietary iron loading. Animals age 6 weeks were fed with modified AIN-76A purified rodent chow with 10,000 ppm (1%) Carbonyl Iron (Dyets Inc., Bethlehem, Pennsylvania) for 10 weeks at Gwathmey Inc. (Cambridge, Massachusetts) before being shipped to our animal facility. Serum iron levels were periodically checked. Before drug administration, serum levels of iron-loaded animals were >2-fold higher (423 μg/dl vs. 187 μg/dl) compared with those in regular chow group. Hepatic iron content was measured in 3 animals in both the regular chow as well as the iron-rich chow fed group. Up to 7-fold elevation (2,397 μg/g vs. 312 μg/g dry weight) in hepatic iron level was observed in iron-loaded animals. This model of dietary carbonyl iron overload is commonly used in experimental work and is known to result in up to 2-fold increase in serum iron and 5- to 8-fold increase in hepatic tissue iron over a period of 12 to 16 weeks (18–20). Increased iron content is seen in liver, spleen, heart, intestinal mucosa, and pancreas, but this does not result in liver cirrhosis (18).

After acclimatization, animals were randomized into treatment groups. Iron-rich diet was maintained throughout the course of the study.

Experimental protocol. DOX TREATMENT. A pilot group (n = 5) of regular chow fed rats was given a single 12 mg/kg body weight intravenous dose of DOX. All animals died within 9 days. Therefore, the dose was scaled down to a single dose of 6 mg/kg. Iron-rich chow fed rats (16 ± 2 weeks old) and regular chow fed rats (14 ± 2 weeks old) were given a single intravenous dose of DOX (6 mg/kg) or saline in their tail veins. Animals were anesthetized 2 to 3 weeks later for imaging, blood sampling, and tissue harvesting (Fig. 1). A mixture of xylazine (10 mg/kg) and ketamine (80 mg/kg) was used at 0.1 ml/100 g (1:10 dilution) of body weight intraperitoneally for anesthesia.

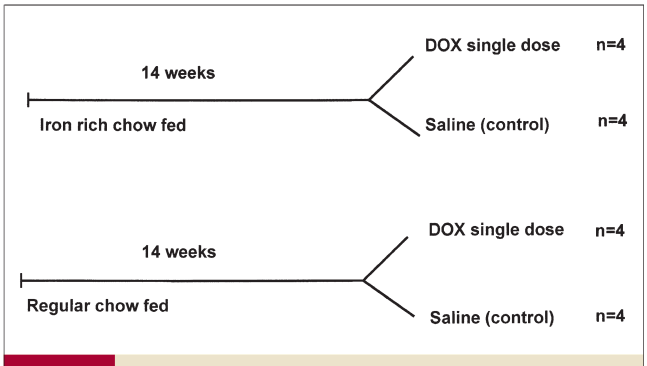

Figure 1 Experimental Protocol

Four animals were included in each experimental as well as control group. DOX = doxorubicin.

Technetium-99m annexin imaging. Human recombinant annexin-V produced by expression in *Escherichia coli* (Apomate, Theseus, Boston, Massachusetts), derivatized with hydrazinonicotinamide (HYNIC, Anor Med, Langley, British Columbia, Canada), and radiolabeled with technetium-99m (^{99m}Tc) (1.0 to 1.2 mCi) (21) was injected in tail veins. Rats were anesthetized 3 h after injection of ^{99m}Tc annexin-V and placed directly on the collimator of a gamma camera (Vertex, Philips Inc., Milipitas, California). Planar whole body images were obtained in prone position using an energy window of 140 ± 20% KeV for 20 min. The images were analyzed visually for the intensity of radiotracer uptake in the hearts. After imaging, the rats were euthanized. Excised hearts were imaged by laying directly on the gamma camera. The hearts were then segmented into 4 regions: apical, subapical, midventricular, and basal. These segments were weighed and counted in an automatic well-type gamma counter for determination of the percent injected dose of ^{99m}Tc annexin-V.

Serial body weight, survival, and gross appearance. Body weight was monitored at baseline and twice a week until the end of the study. General appearances of animals, movement, feeding, social interaction, posture, dehydration, and fur quality were monitored.

The animals that became moribund, lost ≥20% of body weight compared with baseline body weight, and stopped feeding during the course of experiment and were unlikely to survive for more than 1 day had to be euthanized early using a large intraperitoneal dose of pentobarbital.

Determination of myocardial iron content. Myocardial iron content was measured for all animals using acid digestion of myocardial tissue samples followed by iron quantification with atomic spectroscopy (Kansas State University Veterinary Laboratory).

Histopathology and immunohistochemistry. LIGHT MICROSCOPY. Cross sections of heart were cut, fixed in buffered 4% formaldehyde, paraffin embedded, sectioned at 3 to 4 μm, and stained with hematoxylin and eosin and Prussian blue.

HISTOCHEMISTRY. Sections were stained for activated caspase-3 (Biocare Medical, 1:50, Walnut Creek, California) (22). Sections were deparaffinized, blocked with 3% hydrogen peroxide, treated with 1% bovine serum albumin in phosphate-buffered saline, and incubated with the primary antibody at 37°C for 2 h. The specimens were then incubated with horseradish peroxidase-cojugated streptavidin (Biogenex, San Ramon, California) for 10 min and developed with 3,3'diaminobenzidine (Biogenex), and counterstained with hematoxylin. Grading was performed by a blinded reader based on distribution. We created a

scoring system ranging from 0 to 2. Scoring based on distribution was graded on extent of area involved. Less than 30% area involvement was given a score of 0, 30% to 60% a score of 1, and more than 60% was scored as 2.

ELECTRON MICROSCOPY. Small pieces of heart were fixed in half Karnovsky's fixative containing 2.5% glutaraldehyde and 2% paraformaldehyde in 0.1 M phosphate buffer and embedded in epoxy resin, and 40- and 90-nm thick sections were cut with an ultramicrotome, double stained with uranyl acetate and lead citrate, and examined using a transmission electron microscope (Hitachi H-600, Gaithersburg, Maryland).

STATISTICAL ANALYSIS. SPSS/PC 11.0 software was used (SPSS Inc., Chicago, Illinois). Results are expressed in mean ± SEM. Nonparametric tests including Kruskal-Wallis 1-way analysis of variance and Mann-Whitney *U* test were used to compare continuous variables and chi-square for discrete variables. P values <0.05 were considered significant.

Results

All saline-treated control animals survived with normal growth and weight gain with no signs of functional impairment.

Iron-rich chow fed, saline-treated group. Iron-rich chow alone did not result in any deleterious effects with no signs of distress, normal growth, and 100% survival.

DOX treatment in regular chow fed group. Single large intravenous dose of DOX (12 mg/kg) resulted in death within 10 days in all animals (n = 5). Animals showed signs of distress, decreased movement, hunched posture, fuzzy fur, appearance of dark halos around their eyes, and cessation of feeding. Based upon this, 6-mg/kg dose was used in all subsequent single-dose groups. This resulted in a 16% weight loss over 3 weeks compared with 22% weight gain ($p < 0.05$) in corresponding saline-treated control animals over 3 weeks (Fig. 1).

DOX treatment in rats fed iron-rich chow. Six-mg/kg intravenous dose of DOX resulted in a significant and rapid weight loss (18%) over 2 weeks whereas the corresponding DOX-treated animals in regular chow fed group lost 16% weight while both saline-treated control groups fed regular and iron-rich chow gained weight (Fig. 2). Since these animals lost 18% body weight compared with baseline within 2 weeks of receiving DOX and developed severe functional impairment, they had to be sacrificed 1 week earlier than planned.

^{99m}Tc annexin-V imaging. No ^{99m}Tc annexin-V uptake was observed in cardiac regions of regular chow or iron-rich chow fed control groups. Intense cardiac uptake was observed in all DOX-treated groups (Fig. 3). Quantitative cardiac uptake analysis from ex-vivo gamma counting revealed only a minimal uptake in regular chow and iron-rich chow fed animals (Fig. 4). Doxorubicin-treated groups had a significantly higher myocardial uptake. Iron-rich chow fed animals treated with DOX had the highest uptake of ^{99m}Tc annexin-V in cardiac tissue.

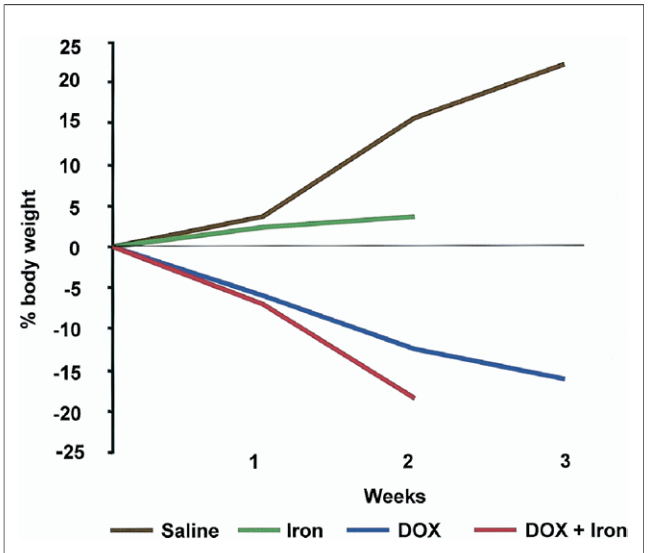

Figure 2 Weight Change

Both iron-rich chow and regular chow fed control animals gained weight. Regular chow fed animals treated with doxorubicin (DOX) showed a progressive weight loss. Weight loss in iron-rich chow group treated with DOX was significantly higher compared with that in other groups.

Myocardial iron content. Feeding iron-rich chow resulted in only a slight increase in myocardial iron content compared with the regular chow fed animals in saline-treated groups (59.00 ± 4.56 μg/g vs. 48.33 ± 7.88 μg/g, p = NS). Myocardial iron contents in the corresponding DOX-treated groups were 70.00 ± 3.08 μg/g vs. 52.25 ± 3.63 μg/g, $p < 0.02$) (23) (Fig. 5).

Histopathology. On light microscopy, no changes were noticed in any group (Fig. 6). Hematoxylin and eosin was remarkably negative for any abnormality. Only rare nonspecific focal inflammatory infiltrates were seen in both DOX-treated regular chow fed and iron-rich chow fed groups. On Prussian blue staining, no stainable iron was seen in any group indicating that increase in myocardial iron content with feeding iron-rich chow was relatively small and well below the levels seen in pathological iron storage conditions.

Electron microscopy showed no cardiac injury in regular chow or iron-rich chow fed control animals (Figs. 7A and 7B). Doxorubicin-treated animal groups had varying grades of injury. Regular chow fed animals showed lesser degree of myofilament loss with DOX treatment (Fig. 7C). More severe changes were seen in iron-rich chow fed animals treated with DOX. Iron-rich chow animals treated with DOX dose had a greater extent of myocyte injury (Fig. 7D). Frequent areas of myofibrillar degeneration and loss, destruction of myocytes, along with mitochondrial and sarcoplasmic swelling and destruction were seen in this group.

Immunohistochemical analysis. Immunostaining using antibodies specific for activated caspase-3 (Fig. 8) revealed distinct positive reaction in all DOX-treated animals. In the group fed regular chow, positive reaction for caspase-3 was

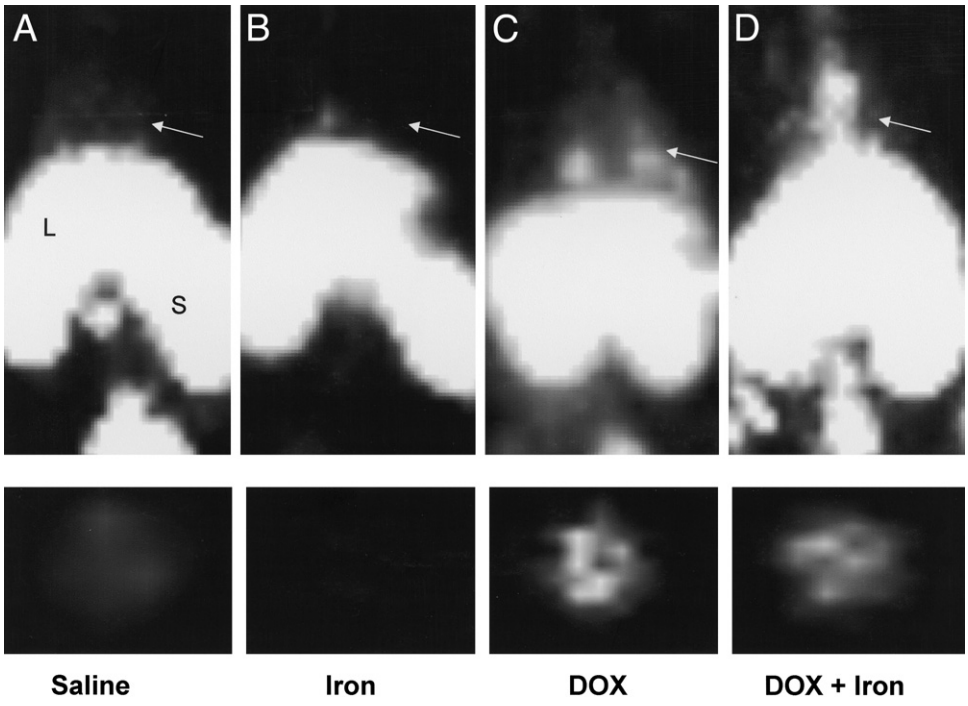

Figure 3 ^{99m}Tc Annexin-V Imaging

Planar whole body **(top)** and ex-vivo images of heart **(bottom)** of animals from each subgroup on ^{99m}Tc annexin-V imaging. There is intense Annexin uptake in liver (L) and spleen (S) with variable uptake in the heart **(arrows)**. No myocardial uptake seen in control group **(A and B)**. Regular chow and iron-rich chow fed animals treated with doxorubicin (DOX) show intense cardiac uptake **(C and D)**.

weaker and focal (grade 1). Animals fed iron-rich chow had a more intense and widespread positive reaction for activated caspase-3 (grade 2). No staining was observed in control animals that received saline, with and without iron-rich chow (grade 0).

Discussion

We employed a rodent model for studying DOX cardiotoxicity and its interaction with iron loading by feeding iron-rich chow for 10 to 14 weeks. Feeding iron-rich chow

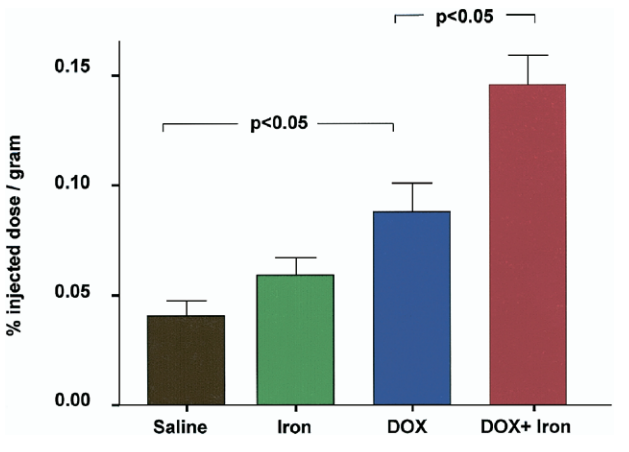

Figure 4 Percent ID/g of Myocardial ^{99m}Tc Annexin-V Uptake

Highest uptake in iron-rich chow fed animals treated with doxorubicin (DOX). ID = injected dose.

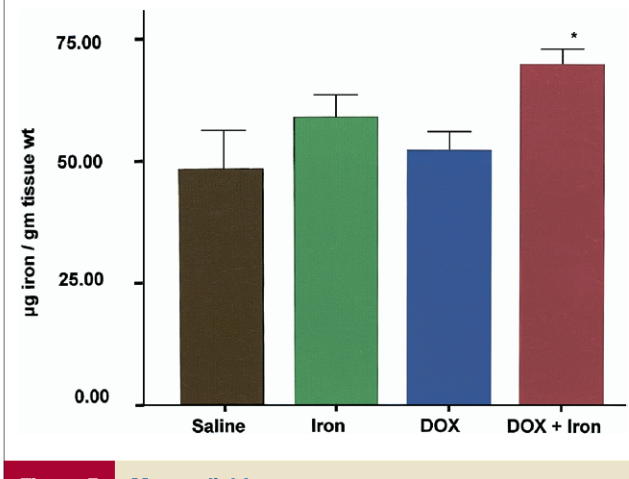

Figure 5 Myocardial Iron

A mild increase in myocardial iron content is seen in iron-rich chow fed animals in both control and doxorubicin (DOX)-treated groups. *$p < 0.05$ compared with DOX and saline.

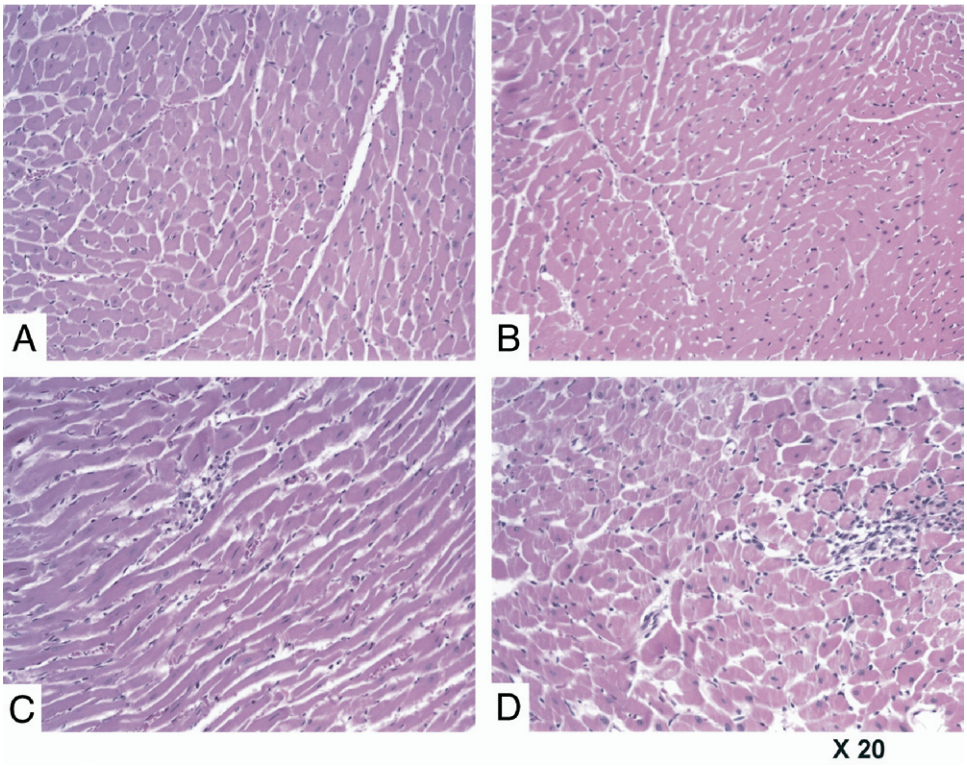

Figure 6 **Light Microscopy**

Light microscopy of hematoxylin- and eosin-stained myocardial tissue shows no signs of myocyte injury in **(A)** regular chow fed animals treated with saline, **(B)** iron-rich chow fed animals treated with saline, **(C)** regular chow fed animals treated with DOX, and **(D)** iron-rich chow fed animals treated with doxorubicin (DOX).

resulted in a profound increase in DOX cardiotoxicity. These animals lost greater body weight. There was greater myocardial ^{99m}Tc annexin uptake in iron-rich chow fed DOX-treated animals compared with that in regular chow fed animals treated with DOX. These findings were confirmed by diffuse and more intense staining of activated caspase-3 on myocardial specimens of iron-rich chow fed animals on DOX treatment. Activated caspase-3 is a sensitive early marker for apoptosis (24). Iron-rich chow alone did not result in any toxicity as seen by effect on body weight, ^{99m}Tc annexin uptake, and absence of signs of injury on histopathological analysis. Light microscopy did not reveal any obvious abnormality among the various groups. This is consistent with previous observations where routine light microscopy was not found to be helpful in detecting or grading the severity of DOX cardiotoxicity (25). Electron microscopy showed most intense degenerative changes in iron-fed DOX-treated animals (Fig 7).

We used ^{99m}Tc annexin-V imaging and activated caspase-3 for studying the intensity of myocardial toxicity in rats. ^{99m}Tc annexin-V imaging has been used for studying other forms of myocardial injury including myocardial infarctions, cardiac transplant rejections (26), and inflammatory myocardial diseases (27). Radiolabeled annexin-V binds to phosphatidylserine, a phospholipid normally present only in inner leaflet of cell membrane that gets exposed on outer cell membrane leaflet in cells undergoing apoptosis. Higher uptake of annexin-V was seen in iron-rich chow fed animals treated with DOX, compared with that seen in regular chow fed animals given DOX.

Mammalian hearts share a susceptibility to DOX cardiotoxicity due to limited protective mechanism from oxidative injury. Heart tissue is relatively deficient in catalase, which, along with glutathione peroxidase, forms the defense against redox injury. The heart primarily depends on glutathione peroxidase to protect itself from free-radical injury. Doxorubicin interferes with glutathione peroxidase making the heart more susceptible to redox injury (28). Doxorubicin-iron complex can catalyze the transfer of electrons from reduced glutathione to molecular oxygen to generate highly reactive superoxide, hydrogen peroxide, and hydroxyl radicals (29).

A number of animal models including mice, rats, dogs, swine, hamsters, and rabbits have been used for studying DOX cardiotoxicity (30,31). We used a rat model because of its suitability for imaging studies and for ease with which nutritional iron overload can be induced in this species. As mentioned earlier, iron overload can be produced by parenteral administration of iron or by feeding chow fortified with iron salts or elemental iron (e.g., carbonyl iron). Parenteral

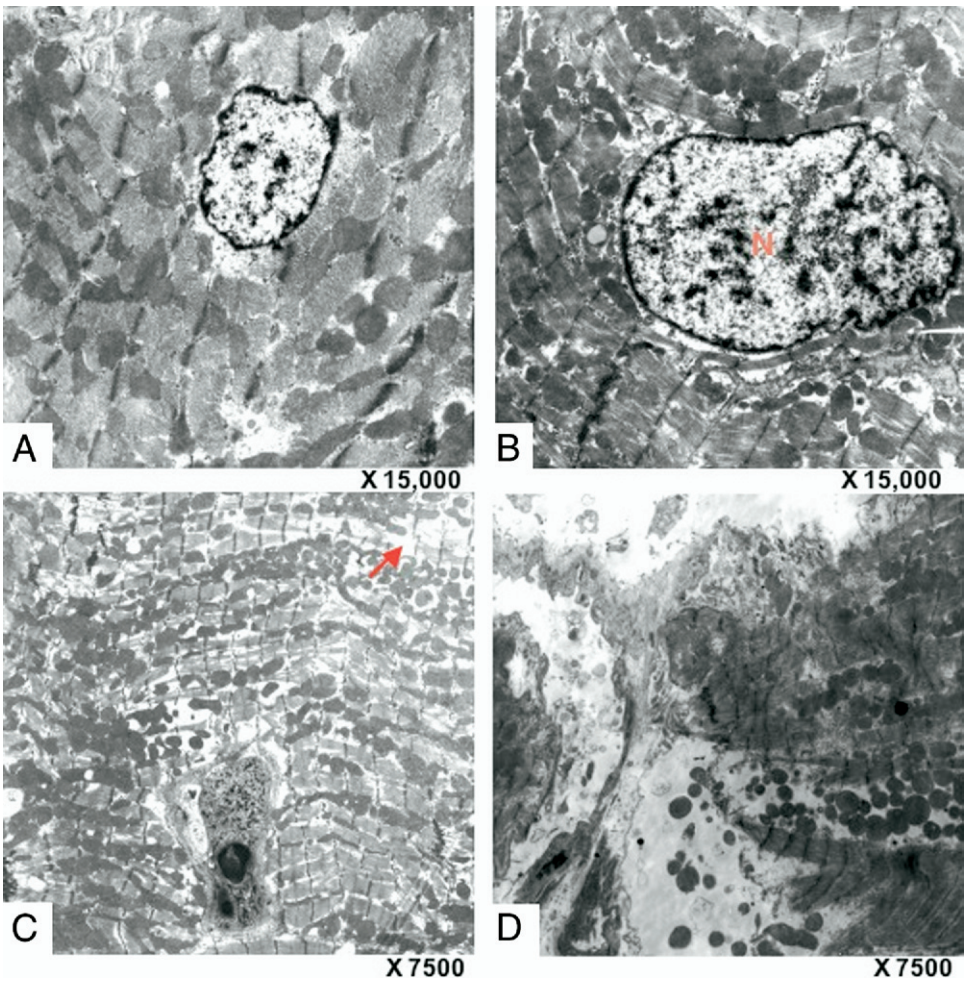

Figure 7 **Electron Microscopy**

(A) No loss of myofilaments is seen in regular chow fed saline-treated animal. **(B)** Minimal myofilament loss in iron-rich chow fed animal treated with saline. **(C)** Regular chow fed doxorubicin-treated animal showed infrequent areas of myofilament loss **(arrow)** without any sarcoplasmic swelling. **(D)** Larger areas of myofilament loss **(arrow)** seen in iron-rich chow fed animals treated with doxorubicin. Iron-rich chow fed animals treated with doxorubicin show frequent and large areas of myofilament loss **(arrow)** accompanied by swelling of sarcoplasmic reticulum, which are characteristic changes seen in doxorubicin cardiotoxicity. N = nucleus.

iron loading results in massive tissue iron overload, with multiorgan damage and toxicity, while oral feeding results only in a relatively modest increase in body iron content without overt signs of end-organ damage. Carbonyl iron is better absorbed and results in less gastrointestinal and systemic toxicity compared with ionic iron (32,33). Dietary carbonyl iron may result in pattern of iron overload similar to that of subclinical iron overload in man. Whereas this mild increase in myocardial iron in saline-treated animals did not result in any obvious cardiotoxicity, this was associated with marked increase in myocyte injury in DOX-treated animals.

To the best of our knowledge, this is the first study to employ a rat model of dietary carbonyl iron overload to assess DOX cardiotoxicity. Doxorubicin cardiotoxicity has been under investigation in humans for well over 3 decades. A number of variables have been considered as contributors to DOX cardiotoxicity (6). Even while iron has been reported to play a role in DOX cardiotoxicity in experimental studies (13,34,35), importance of iron as an independent variable has not been studied in humans. A wide variation can occur in body iron stores in patients undergoing cancer chemotherapy, depending upon abnormal blood losses, blood transfusions, iron supplementation, and nutritional status. Adult and pediatric patients undergoing treatment for leukemia and other malignancies can develop a significant level of iron overload during and as a result of chemotherapy and bone marrow transplantation (36). It has also been observed that iron level may predict outcomes in cancer survivors. Level of iron overload observed varies between moderate to severe levels in 15% to 20% of long-term survivors (37–39). Several common genetic disorders may also influence body iron stores. Hemochromatosis, the most common form of genetic disorder of iron

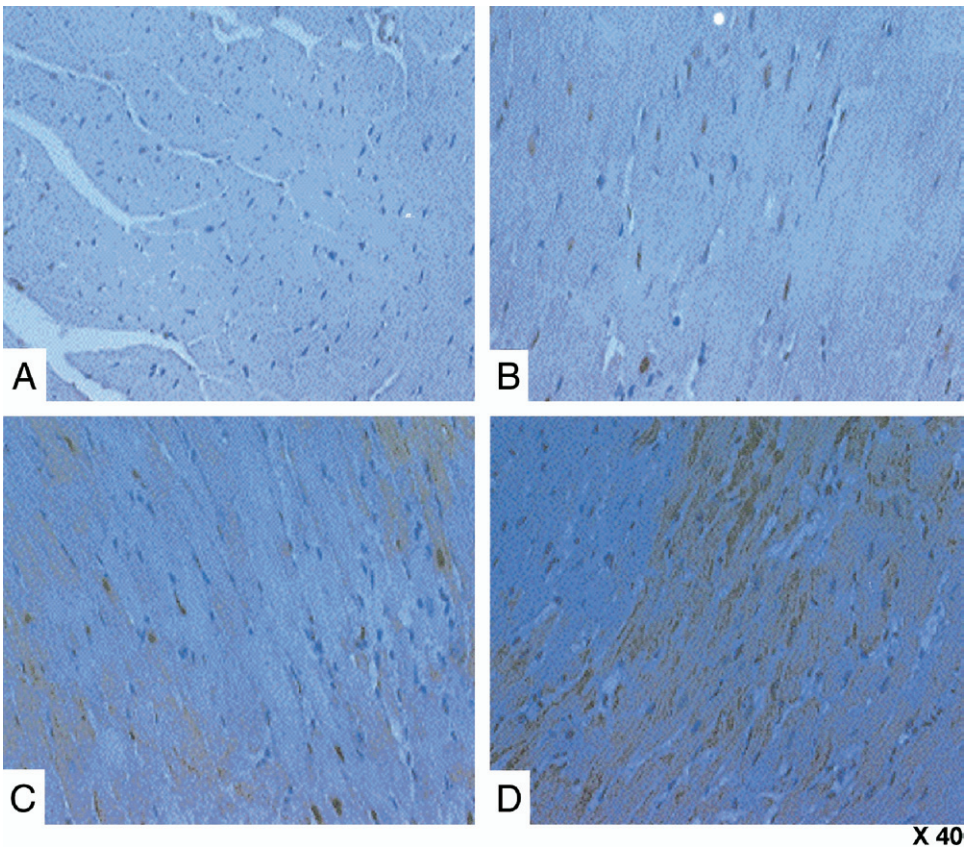

Figure 8 **Activated Caspase-3 Immunohistochemistry of Myocardial Specimens**

Activated caspase-3 was present in the cytoplasm of cells with morphology consistent with apoptosis. Positive staining is seen in myocardium of animals treated with doxorubicin **(C and D)**. No staining is seen in control animals fed **(A)** regular chow or **(B)** iron-rich chow. Iron-rich chow fed animals treated with doxorubicin **(D)** show a greater area of staining involving higher number of myocytes compared with regular chow fed animals treated with doxorubicin **(C)**.

overload, has a frequency of 1:250 to 400 in Americans of Northern European descent. This is characterized by homozygous mutation ($C282Y^{+/+}$) of iron regulatory gene (HFE gene) resulting in unregulated intestinal absorption of iron. However, heterozygous prevalence of this gene ($C282Y^{+/-}$) is very common in the same population (7% to 8%) (40). Another mutation of the HFE gene associated with milder degree of iron overload ($H63D^{+/-}$) has a prevalence of up to 20% (40). Heterozygous carriers of these mutations may have subclinical and otherwise asymptomatic increase in body iron stores. Dexrazoxane, the only chelator used clinically in patients, is recommended for use beyond a cumulative DOX dose of 300 mg/m^2 (17). As toxicity may begin much earlier, in the presence of elevated body iron, perhaps this agent may be considered earlier during the course of DOX or even before DOX therapy in those with elevated body iron stores.

Our findings are similar to those of Miranda et al. (41) who recently observed increased susceptibility to DOX cardiotoxicity in HFE knockout mice. They observed higher mortality, greater increase in creatine kinase and aminotransferase enzymes, and more severe histologic change in the HFE knockout mice compared with that in wild type. Both of these studies emphasize the critical role of iron in DOX cardiotoxicity. However, Corna et al. (42) reported a paradoxical benefit between anthracycline-derived reactive oxygen species, increased ferritin synthesis, and resistance to iron-mediated damage. Authors reported protection of H9c2 cells from ferric ammonium citrate-induced damage on pretreatment with DOX by down-regulating iron regulatory protein-2 and subsequent increase in ferritin synthesis. The role of iron and reactive oxygen species in anthracycline-induced cardiotoxicity may, therefore, be more complex than previously believed (42). However, these findings need further study and are contrary to our findings of increased cardiac injury in iron-supplemented animals receiving DOX.

We speculate that higher body iron stores in patients who have received multiple blood transfusions, prolonged iron supplementation, or those with unsuspected HFE mutations may be predisposed to DOX cardiotoxicity. Prospective clinical studies are needed to test our hypothesis. If these results are confirmed by clinical studies, simple and relatively inexpensive screening tests for total body iron

stores and presence of HFE mutation can be used to screen patients before initiating DOX chemotherapy.

Acknowledgment
The authors thank Mr. Gunner Snyder for his help with nuclear imaging.

Reprint requests and correspondence: Dr. Diwakar Jain, Drexel University College of Medicine, 245 North 15 Street, MS 470, Philadelphia, Pennsylvania 19102. E-mail: Diwakar.Jain@drexelmed.edu.

REFERENCES

1. Hortobagyi GN. Anthracyclines in the treatment of cancer. An overview. Drugs 1997;54 Suppl 4:1–7.
2. Shan K, Lincoff AM, Young JB. Anthracycline-induced cardiotoxicity. Ann Intern Med 1996;125:47–58.
3. Lipshultz SE, Rifai N, Dalton VM, et al. The effect of dexrazoxane on myocardial injury in doxorubicin-treated children with acute lymphoblastic leukemia. N Engl J Med 2004;351:145–53.
4. Jain D. Cardiotoxicity of doxorubicin and other anthracycline derivatives. J Nucl Cardiol 2000;7:53–62.
5. Keefe DL. Anthracycline-induced cardiomyopathy. Semin Oncol 2001;28:2–7.
6. Mitani I, Jain D, Joska TM, Burtness B, Zaret BL. Doxorubicin cardiotoxicity: prevention of congestive heart failure with serial cardiac function monitoring with equilibrium radionuclide angiocardiography in the current era. J Nucl Cardiol 2003;10:132–9.
7. Muller I, Niethammer D, Bruchelt G. Anthracycline-derived chemotherapeutics in apoptosis and free radical cytotoxicity (review). Int J Mol Med 1998;1:491–4.
8. Singal PK, Li T, Kumar D, Danelisen I, Iliskovic N. Adriamycin-induced heart failure: mechanism and modulation. Mol Cell Biochem 2000;207:77–86.
9. Gewirtz DA. A critical evaluation of the mechanisms of action proposed for the antitumor effects of the anthracycline antibiotics adriamycin and daunorubicin. Biochem Pharmacol 1999;57:727–41.
10. Yourtee DM, Elkins LL, Nalvarte EL, Smith RE. Amplification of doxorubicin mutagenicity by cupric ion. Toxicol Appl Pharmacol 1992;116:57–65.
11. Colombo R, Dalle Donne I, Milzani A. Metal ions modulate the effect of doxorubicin on actin assembly. Cancer Biochem Biophys 1990;11:217–26.
12. Chakrabarti S, Mahmood A, Kassis AI, Bump EA, Jones AG, Makrigiorgos GM. Generation of hydroxyl radicals by nucleohistone-bound metal-adriamycin complexes. Free Radic Res 1996;25:207–20.
13. Myers C. The role of iron in doxorubicin-induced cardiomyopathy. Semin Oncol 1998;25:10–4.
14. Gianni L, Myers CE. The role of free radical formation in the cardiotoxicity of anthracycline. In: Muggia FM, Green MD, Speyer JL, editors. Cancer Treatment and the Heart. 1st edition. Baltimore, MD: Johns Hopkins University Press, 1992:9–46.
15. Malisza KL, Hasinoff BB. Production of hydroxyl radical by iron(III)-anthraquinone complexes through self-reduction and through reductive activation by the xanthine oxidase/hypoxanthine system. Arch Biochem Biophys 1995;321:51–60.
16. Wiseman LR, Spencer CM. Dexrazoxane. A review of its use as a cardioprotective agent in patients receiving anthracycline-based chemotherapy. Drugs 1998;56:385–403.
17. Schuchter LM, Hensley ML, Meropol NJ, Winer EP. 2002 update of recommendations for the use of chemotherapy and radiotherapy protectants: clinical practice guidelines of the American Society of Clinical Oncology. J Clin Oncol 2002;20:2895–903.
18. Iancu TC, Ward RJ, Peters TJ. Ultrastructural observations in the carbonyl iron-fed rat, an animal model for hemochromatosis. Virchows Arch B Cell Pathol Incl Mol Pathol 1987;53:208–17.
19. Kang JO, Jones C, Brothwell B. Toxicity associated with iron overload found in hemochromatosis: possible mechanism in a rat model. Clin Lab Sci 1998;11:350–4.
20. Plummer JL, MacKinnon M, Cmielewski PL, et al. Dose-related effects of dietary iron supplementation in producing hepatic iron overload in rats. J Gastroenterol Hepatol 1997;12:839–42.
21. Blankenberg FG, Katsikis PD, Tait JF, et al. In vivo detection and imaging of phosphatidylserine expression during programmed cell death. Proc Natl Acad Sci U S A 1998;95:6349–54.
22. Gown AM, Willingham MC. Improved detection of apoptotic cells in archival paraffin sections: immunohistochemistry using antibodies to cleaved caspase 3. J Histochem Cytochem 2002;50:449–54.
23. Edwards CQ. Hemochromatosis. In: Greer JP, Foerster J, editors. Wintrobes's Clinical Hematology. 11th edition. Philadelphia, PA: Lippincott Williams & Wilkins, 2004:979–1050.
24. Duan WR, Garner DS, Williams SD, Funckes-Shippy CL, Spath IS, Blomme EA. Comparison of immunohistochemistry for activated caspase-3 and cleaved cytokeratin 18 with the TUNEL method for quantification of apoptosis in histological sections of PC-3 subcutaneous xenografts. J Pathol 2003;199:221–8.
25. Isner JM, Ferrans VJ, Cohen SR, et al. Clinical and morphologic cardiac findings after anthracycline chemotherapy. Analysis of 64 patients studied at necropsy. Am J Cardiol 1983;51:1167–74.
26. Narula J, Acio ER, Narula N, et al. Annexin-V imaging for noninvasive detection of cardiac allograft rejection. Nat Med 2001;7:1347–52.
27. Strauss HW, Grewal RK, Pandit-Taskar N. Molecular imaging in nuclear cardiology. Semin Nucl Med 2004;34:47–55.
28. Doroshow JH, Locker GY, Baldinger J, Myers CE. The effect of doxorubicin on hepatic and cardiac glutathione. Res Commun Chem Pathol Pharmacol 1979;26:285–95.
29. Myers CE, Gianni L, Simone CB, Klecker R, Greene R. Oxidative destruction of erythrocyte ghost membranes catalyzed by the doxorubicin-iron complex. Biochemistry 1982;21:1707–12.
30. Herman EH, Ferrans VJ. Preclinical animal models of cardiac protection from anthracycline-induced cardiotoxicity. Semin Oncol 1998;25:15–21.
31. Imondi AR, Della Torre P, Mazue G, et al. Dose-response relationship of dexrazoxane for prevention of doxorubicin-induced cardiotoxicity in mice, rats, and dogs. Cancer Res 1996;56:4200–4.
32. Huebers HA, Brittenham GM, Csiba E, Finch CA. Absorption of carbonyl iron. J Lab Clin Med 1986;108:473–8.
33. Crosby WH. Prescribing iron? Think safety. Arch Intern Med 1978;138:766–7.
34. Hershko C, Link G, Tzahor M, et al. Anthracycline toxicity is potentiated by iron and inhibited by deferoxamine: studies in rat heart cells in culture. J Lab Clin Med 1993;122:245–51.
35. Hasinoff BB, Davey JP. The iron(III)-adriamycin complex inhibits cytochrome c oxidase before its inactivation. Biochem J 1988;250:827–34.
36. Barton JC, Bertoli LF. Transfusion iron overload in adults with acute leukemia: manifestations and therapy. Am J Med Sci 2000;319:73–8.
37. Lichtman SM, Attivissimo L, Goldman IS, Schuster MW, Buchbinder A. Secondary hemochromatosis as a long-term complication of the treatment of hematologic malignancies. Am J Hematol 1999;61:262–4.
38. Harrison P, Neilson JR, Marwah SS, Madden L, Bareford D, Milligan DW. Role of non-transferrin bound iron in iron overload and liver dysfunction in long term survivors of acute leukaemia and bone marrow transplantation. J Clin Pathol 1996;49:853–6.
39. Halonen P, Mattila J, Suominen P, Ruuska T, Salo MK, Makipernaa A. Iron overload in children who are treated for acute lymphoblastic leukemia estimated by liver siderosis and serum iron parameters. Pediatrics 2003;111:91–6.
40. Steinberg KK, Cogswell ME, Chang JC, et al. Prevalence of C282Y and H63D mutations in the hemochromatosis (HFE) gene in the United States. JAMA 2001;285:2216–22.
41. Miranda CJ, Makui H, Soares RJ, et al. Hfe deficiency increases susceptibility to cardiotoxicity and exacerbates changes in iron metabolism induced by doxorubicin. Blood 2003;102:2574–80.
42. Corna G, Santambrogio P, Minotti G, Cairo G. Doxorubicin paradoxically protects cardiomyocytes against iron-mediated toxicity: role of reactive oxygen species and ferritin. J Biol Chem 2004;279:13738–45.